Mem. S.A.It. Vol. 83, 162

Memorie della

Multi-wavelength observations of H.E.S.S. AGN

M. Tluczykont[1] for the H.E.S.S. Collaboration[2]

[1] Institut für Experimentalphysik, Universität Hamburg, Luruper Chaussee 149, 22761, Hamburg, Germany
[2] http://www.mpi-hd.mpg.de/hfm/HESS/pages/collaboration/
e-mail: martin.tluczykont@physik.uni-hamburg.de

Abstract. Multi-frequency observations are a powerful tool of astrophysical investigation. Not only is data in each wavelength band providing different clues to the objects nature, but taken simultaneously, these data can reveal the mechanisms at work in astrophysical objects. In the past years, joint multi-frequency observations with the H.E.S.S. telescopes in the very high energy (VHE, E>100 GeV) band and several other experiments in the radio, optical, X-ray, and high energy (HE, E>100 MeV) bands have lead to intriguing results that will ultimately help answering the open questions of the location of the very high energy emission, details of the acceleration mechanism, and the role of the central black hole.

Key words. Galaxies: active – Gamma rays: observations – X-rays: galaxies

1. Introduction

Very high energy (VHE, E>100 GeV) gamma-ray astronomy is the domain of Earth-bound air-shower experiments. The direction, energy and particle type (gamma-hadron separation) can be reconstructed via the measurement of air-shower particles, or by Cherenkov photons emitted by them. Imaging air Cherenkov telescopes (IACTs) make an image of the shower in Cherenkov light.

In the last decade, the IACT technique has made the step from the pioneering era, dominated by experiments such as Whipple, HEGRA, CAT, or CANGAROO, to the now ongoing first physics era, with H.E.S.S. (Aharonian et al. 2006a), MAGIC (Albert et al. 2008), and VERITAS (Acciari et al. 2008). As compared to the non-imaging technique, advantages of IACTs are their good angular resolution ($< 0.1°$), a relative energy resolution around 15 %, a low energy threshold (E > 100 GeV for a 100 m^2 mirror dish) and a very good sensitivity to point-like sources. Today, Crab Nebula like sources can be detected in the VHE regime in ~30 s (5 σ significance level). As compared to the previous generation of IACTs, a significant leap forward has been achieved. Not only has the number of known Galactic and extragalactic VHE sources sharply increased, see e.g. Giebels et al. (2010) for an overview, or Raue (2011) for recent H.E.S.S. results. The quality of the measurements also improved to the point of resolving lightcurves down to the minute timescale, spectra extending from 100 GeV to beyond 10 TeV, and sensitivities allowing to detect VHE emission from quiescent AGN (see below).

The H.E.S.S. experiment is an array of four IACTs located in Namibia in the Khomas

Send offprint requests to: M. Tluczykont highlands, for observations of Galactic and extragalactic sources in the energy range from 100 GeV to several 10 TeV.

AGN are an ideal target for multi-frequency observations. Their spectral energy distribution (SED) reaches from radio waves via optical, X-rays, to very-high-energies. In the widely-accepted unified model of AGN (e.g. Rees 1984; Urry & Padovani 1995), the "central engine" of these objects consists of a thin accretion disk of gas, accreting onto a super-massive central black hole (up to $10^9\,M_\odot$), and surrounded by a dust torus. In radio-loud AGN, i.e. objects with a radio to B-band flux ratio $F_{5GHz}/F_B > 10$, two relativistic plasma outflows (jets) presumably perpendicular to the plane of the accretion disk have been observed. AGN are known to be VHE γ-ray emitters since the detection of Mrk 421 above 300 GeV by the Whipple group (Punch et al. 1992). Almost all AGN that were detected in the VHE regime belong to the class of BL Lac objects, i.e. AGN having their jet pointing at a small angle to the line of sight. VHE gamma-rays were also detected from two radio galaxies, M 87 (see below), and Cen A (Aharonian et al. (2009c), also see Rieger (2011), these proceedings), the starburst galaxy NGC 253 (Acero et al. 2009) and the FSRQs 3C279 (Aleksić et al. 2011a) and PKS 1222+21 (Aleksić et al. 2011b).

The characteristic two-peak SED of AGN can be explained by synchrotron emission of relativistic electrons, and an inverse Compton (IC) peak, resulting from scattering of electrons off a seed-photon population, see e.g. Sikora & Madejski (2001) and references therein. Alternatively, hadronic radiation models explain the emission via the interactions of relativistic protons with matter (Pohl & Schlickeiser 2000), ambient photons (Mannheim 1993) or magnetic field (Aharonian 2000), or photons and magnetic field (Mücke & Protheroe 2001). The observed VHE emission shows high variability ranging from short bursts on a minute time-scale, to long-term activity of the order of months. Studies of the variability of BL Lac type objects can contribute to the understanding of their intrinsic acceleration mechanisms (e.g. Krawczynski et al. 2001; Aharonian et al. 2002). VHE gamma-rays can be absorbed via e^+e^- pair production with the photons of the extragalactic background light (EBL). Observations of distant objects in the VHE band therfore provide an indirect measurement of the SED of the EBL, see e.g. Stecker et al. (1992); Primack et al. (1999) and references therein. Open questions of VHE emission in AGN persist:

- where in the jet does gamma-ray emission occur? While it is believed that the VHE emission must be beamed and thus originate somewhere along the jet axis, the exact location is still unknown.
- What is the source of the soft seed photons for the inverse Compton effect? Seed photon fields can originate in different regions, such as the accretion disk, different parts of the jet, the broad line region, the dusty torus, and synchrotron photons. The latter are favoured, considering the practically feature-less spectra in the optical and ultra-violet, and for the sake of gamma-ray transparency (local radiation fields must be low enough to avoid intrinsic absorption by pair production).
- Finally, what is the role of the central black hole in powering the jet? The transfer of binding energy of accreting gas to the jet as well as spin-energy extraction via the Blandford-Znajek mechanism (Blandford & Znajek 1977) are discussed.

2. Multi-frequency observations

2.1. Overview

A number of AGN were observed by H.E.S.S. since the start of operation in 2002. Some sources were observed in the frame of organized multi-frequency campaings, or regular monitoring campaigns, while others were triggered by high-state observations reported by other instruments. Table 1 gives an overview of H.E.S.S. observations of AGN for which simultaneous multi-frequency data was taken.

Table 1. Summary of published simultaneous multi-wavelength data sets of H.E.S.S. AGN.

Object	Years	MWL	arXiv:astro-ph/ or reference
PKS 2155-304	2003,-06,-08	RXTE, ROTSEIII, NRT, Bronberg opt. RXTE, Chandra, Swift, ATOM	0506593v1, 0906.2002v1, 0903.2924v1
H 2356-309	2004-2007	RXTE, ROTSEIII, NRT XMM, ATOM, NRT	0607569v1, 1004.2089v2
PKS 2005-489	2004-2007	XMM-Newton, RXTE	0911.2709v2
1ES 1101-232	2004,2005	XMM-Newton, RXTE, optical	07052946v2
Mrk 421	2004	RXTE	0506319v1
1ES 0347-121	2006	Swift	0708.3021v1
PG 1553+113	2005/2006	VLT (SINFONI)	0710.5740v2
RGB J0152+017	2007	RXTE, Swift, ATOM	0802.4021v2
PKS0548-322	2004-2008	Swift	1006.5289v2
M 87	2003-2008	Chandra, VLBA	Aharonian et al. (2006d) Acciari et al. (2009)
AP Librae	2010	Swift, RXTE, Fermi	Fortin et al. (2011)
HESS J1943+213	2011	Fermi, NRT	1103.0763v1

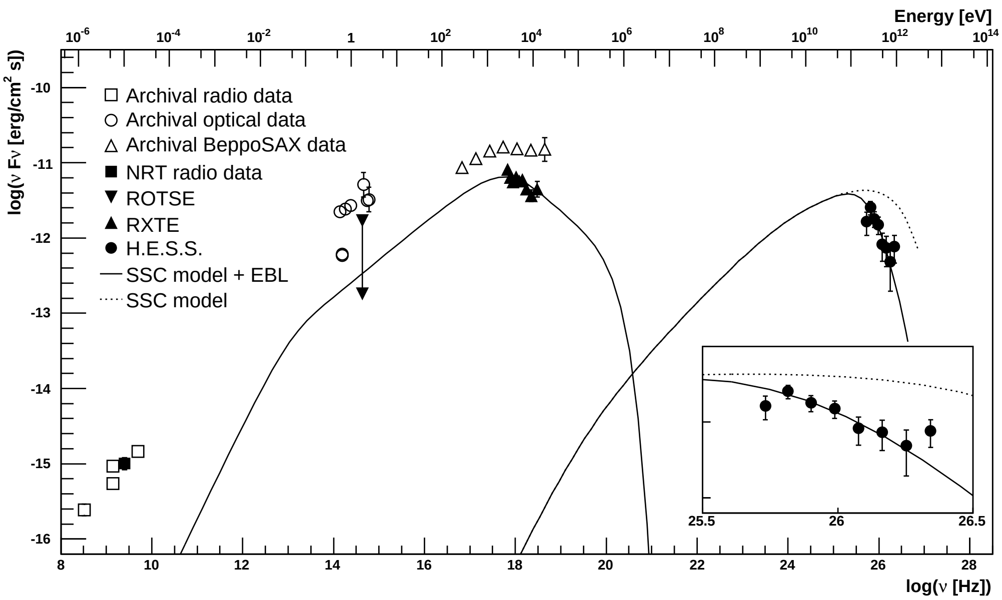

Fig. 1. Historically, this SED of H 2356−309 from 2004 was the first SED comprising simultaneous radio, optical, X-ray and VHE observations. Simultaneous data are shown as filled symbols. All other (archival) data are shown as open symbols. Radio emission arises from regions further out in the jet. A single-zone SSC model taking absorption into account is shown as a solid line (dashed line without absorption).

2.2. H 2356-309 and 1ES 1101-232

The high frequency peaked BL Lac object (HBL) H 2356−309 (z = 0.165) was first identified at optical frequencies by Schwartz et al. (1989). Its first detection in the X-ray band was done by satellite experiment UHURU (Forman et al. 1978). Later observations with BeppoSAX established it as an *extreme synchrotron blazar* (Costamante et al. 2001). H 2356−309 was discovered in the VHE gamma-ray regime by H.E.S.S. after observations in 2004 (Aharonian et al. 2006b). Simultaneous observations were carried out with RXTE in X-rays on 11th of November 2004, with the Nançay decimetric radio telescope (NRT) between June and October 2004 and with ROTSE in the optical, covering the whole 2004 H.E.S.S. observation campaign. With these data for the first time, an SED comprising simultaneous radio, optical, X-ray and VHE measurements could be made. The resulting broad-band SED from this observation campaign (Figure 1) can be well described by a single-zone synchrotron self Compton (SSC) model, using a reasonable set of parameters. A later multi-frequency campaign (HESS Collaboration et al. 2010) with H.E.S.S., NRT, ATOM, and XMM-Newton, yielded similar results. The object still showed little variability (factor 2) and was in a historically low X-ray-level. A similar case of a broad-band SED compatible with a single-zone SSC model is given by multi-frequency observations of the extreme synchrotron blazar 1ES 1101-232 (Aharonian et al. 2007b). Due to their comparatively large redshift, the results obtained from H 2356−309 and 1ES 1101−232 (z = 0.186) lead to strong constraints on the density of the EBL (Aharonian et al. 2006c).

2.3. PKS 2155−304

The high frequency peaked BL Lac object PKS 2155−304 (z = 0.117) is one of the best studied blazars in the southern hemisphere. After first being detected in the X-ray band (Cooke et al. 1978; Griffiths et al. 1979; Schwartz et al. 1979), it was detected in the VHE regime by the *University of Durham Mark 6 Telescope* in 1996 and 1997 (Chadwick et al. 1999). H.E.S.S. could confirm these findings in early observations before the completion of the experiment in 2002 and 2003 (Aharonian et al. 2005a). In a subsequent multi-frequency campaign in 2003 (Aharonian et al. 2005b), the object was observed in a hisorically low flux level in X-rays. Furthermore, the weak variability in the VHE H.E.S.S. data (smaller than factor 2.5) and the notable fact that PKS 2155−304 was detectable within each observation night by H.E.S.S. indicated that the object was observed in a quiescent flux state. Simultaneous multi-frequency observations in 2008 (Aharonian et al. 2009b, H.E.S.S., Fermi, RXTE, and ATOM) yielded a clear optical/VHE correlation and evidence for a correlation of the X-ray flux with the spectral index in the high energy regime (Fermi data, E>100 MeV). A behaviour that is difficult to explain in the framework of SSC models.

The most notable events concerning this source, however, did happen in two exceptionally bright VHE outbursts in 2006 (Aharonian et al. 2007a, 2009a). In the first observation night covered by H.E.S.S., variability could be detected at the minute time-scale (3 min bins). Assuming a size of the emission region of the order of the Schwarzschild radius, causality requires a Doppler factor of more than 100 in order to accomodate the observed fast variability. As shown by Degrange et al. (2008), the data show log-normal flux variability in the VHE regime (also seen in Mrk 421, Tluczykont et al. 2010). Such a variability pattern is indicative of a multiplicative process, implying a connection of the VHE emission to accretion disk activity (see Giebels & Degrange 2009, and references therein). Furthermore, a log-normal flux behaviour is incompatible with an additive process such as a multi-zone IC emission scenario.

As opposed to the first observation night, the second H.E.S.S. observation night (Aharonian et al. 2009a) was also covered by observations by Chandra (and partly by RXTE and Swift) in X-rays, and the Bronberg optical observatory. A clear VHE/X-ray correlation was found, without significant timelags between both frequency bands. The main variability structure and sub-structures of the VHE lightcurves are matched in X-rays. However, rapid sub-flares observed in the VHE band are not found in the Chandra data. Huge differences in the variability amplitudes of ~10/2/1.15 were observed between the VHE/X-ray/optical bands. The ratio of VHE (inverse Compton) to X-ray (synchrotron) flux was at a maximum of 8 during the decaying phase of the flare, and reached a minimum at the end of the observation night. Such a high and rapidly varying *Compton dominance* was never observed before.

Spectral analysis of the H.E.S.S. data show a curved spectrum with a stronger curvature at high flux states, indicating that the observed curvature is at least partly intrinsic. Overall, the spectral index shows a harder-when-brighter relationship in the VHE regime. While such a dependency is also seen in the simultaneous Chandra data, the partly sampled X-ray flare starting after the H.E.S.S. exposure shows a softer-when-brighter relation.

Remarkably, the gamma-ray flux traces the variations of the X-ray flux much stronger than quadratically (Figure 2). Instead, a cubic relation is found. As discussed in Aharonian et al. (2009a), such a super-quadratic relationship is challenging common scenarios of VHE emission in blazars.

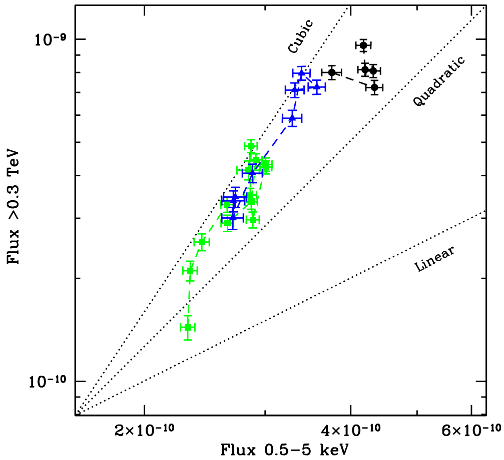

Fig. 2. Correlation between X-ray and VHE flux during 3 different states of the second exceptional flare (MJD53946): maximum (black), decaying phase (blue), and broad sub-flare (green). Mostly, a cubic relationship between the VHE and X-ray bands is observed.

2.4. M 87

The giant radio galaxy M 87 ($z = 0.0043$) is located at the center of the Virgo cluster of galaxies, and hosts a central black hole of $(3.2 \pm 0.9)\cdot10^9\,M_\odot$. As opposed to blazars, the jet of M 87 is orientated at an angle of $\approx 30°$ relative to the line of sight. The possibility of multi-frequency observations with radio instruments that are able to resolve substructures of its jet make M 87 a very interesting object for studying the location of the VHE emission. After first indications for a VHE signal in HEGRA data (Aharonian et al. 2003), H.E.S.S. observations between 2003 and 2006 could establish M 87 as the first VHE emitting radio galaxy (Aharonian et al. 2006d). The spectrum seen by H.E.S.S. is well described by a pure powerlaw. The hardness (spectral index 2.22 ± 0.15 in 2005) of the observed spectrum extending beyond 10 TeV and the lack of any absorption feature due to pair production imply a low central infra-red (IR) luminosity at 0.1 eV (10 μm), as could be expected in the case of an advection-dominated accretion disk. It also excludes significant contributions of the IR radiation fields as external seed photon population. While the position of the VHE excess rules out the radio lobes as potential site for the gamma-ray production, the resolution of the H.E.S.S. Cherenkov telescopes does not allow to resolve structures smaller than the large scale lobe structure of M 87. However, the unexpectedly fast variability observed in H.E.S.S. data from 2005 allowed to strongly constrain the size of the emission region. Several potential sites and mechanisms for VHE gamma-ray production could thus be excluded: the elliptical host galaxy, dark matter, the kpc-scale jet, and the brightest knot (knot A) in the jet (see Aharonian et al. 2006d, for discussion). Remarkably, simultaneous observations carried out with the *Chandra* satellite showed that the highest VHE flux state observed by H.E.S.S. coincided with a maximum X-ray flux from the HST-1 hotspot.

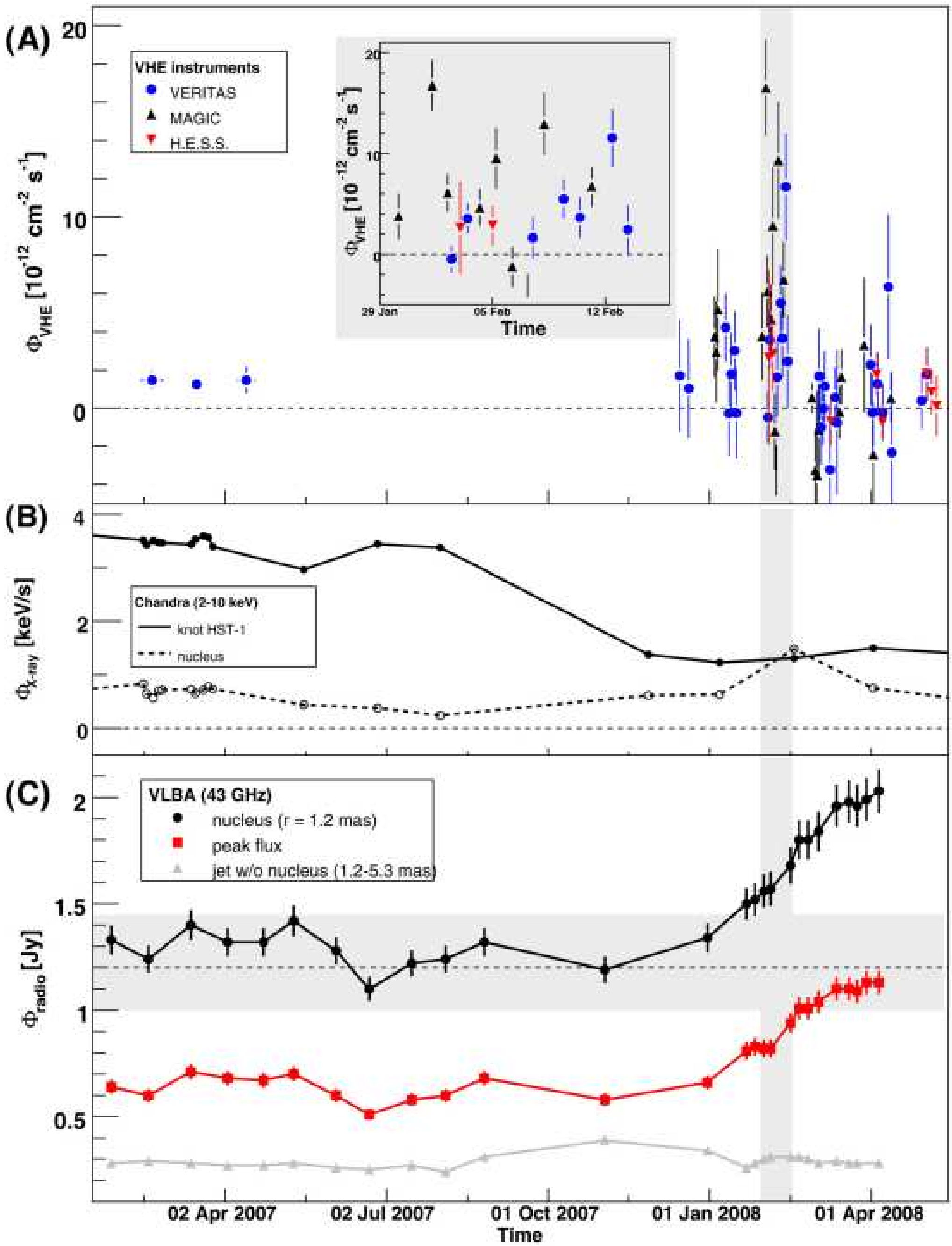

Fig. 3. Light curves for M 87 (2007–2008) (from Acciari et al. 2009). (A) nightly VHE gamma-ray fluxes (E>0.35 TeV). (B) Chandra X-ray data (2 to 10 keV) of the nucleus and the knot HST-1 (Harris et al. 2009). (C) Flux densities from the 43-GHz VLBA observations of the nucleus, the peak flux, and the flux integrated along the jet. For details, see (Acciari et al. 2009).

In order to bypass the poor angular resolution of IACTs, a multi-frequency campaign was carried out with participation of VERITAS, MAGIC, and H.E.S.S., together with the Very Long Baseline Array (VLBA) at 43 GHz with a resolution of 0.21×0.43 mas, and Chandra in the X-ray band (Acciari et al. 2009). As opposed to the previous findings by H.E.S.S., the VHE maximum observed by all IACTs in 2008 occured during a minimum of X-ray activity from HST-1 (see Figure 3). Instead, the VLBA data shows that the VHE flare occurs during a rise of activity in the nucleus. These findings are an indication for the VHE emission to be taking place in the jet collimation region (see Acciari et al. 2009). Recent data on M 87 show an even more intriguing multi-frequency picture (see e.g. Raue 2011).

3. Summary

In the past decade, observations with H.E.S.S. and other instruments in other wavelength bands have produced pieces of the puzzles of VHE emission from AGN (See open questions, Introduction, page 162).

A log-normal flux pattern (multiplicative process) found in the VHE data of PKS 2155-304 (and in combined data on Mrk 421) might hint at a connection of the VHE emission to accretion disk activity, and are contradictory to an additive multi-zone IC scenario. During the second exceptional flare of PKS 2155-304 observed by H.E.S.S., a cubic relationship was found between the X-ray flux and the VHE flux, challenging common models of IC emission. The unprecedentedly fast variability (minute time-scale) seen from this source strongly constrains the size of the VHE emission region. A comparatively fast variability of the order of days was also found in H.E.S.S. data on the radio galaxy M 87, ruling out several hypotheses for the location of the VHE emission region. In a VHE/X-ray/radio multi-frequency campaign, evidence was found for a connection of the VHE emission from M 87 to the jet collimation region.

4. Discussion

SERGIO COLAFRANCESCO: It seems that the radio high-resolution observations are crucial for the location of the VHE emission. Do you also have radio polarization observations to better identify the radio blob responsible for the VHE emission ?

MARTIN TLUCZYKONT: We don't have results from polarization measurements yet. P.S.: during the session, the answer referred to results instead of existence of data. Data exist and analysis is in progress.

JIM BEALL: Can you comment on the size scale where the VHE / radio emission occurs ?

MARTIN TLUCZYKONT: From causality arguments alone, the fast variability observed from M 87 implies an absolute *size* of the emission region of the order of 3 Schwarzschild radii of the central black hole (3×10^{15} cm). The absolute *position* of the VHE emission can be derived to be within the jet collimation region, considering the simultaneity of the VHE flare with the radio emission from the nucleus in 2008.

Acknowledgements. The support of the Namibian authorities and of the University of Namibia in facilitating the construction and operation of H.E.S.S. is gratefully acknowledged, as is the support by the German Ministry for Education and Research (BMBF), the Max Planck Society, the French Ministry for Research, the CNRS-IN2P3 and the Astroparticle Interdisciplinary Programme of the CNRS, the U.K. Science and Technology Facilities Council (STFC), the IPNP of the Charles University, the Polish Ministry of Science and Higher Education, the South African Department of Science and Technology and National Research Foundation, and by the University of Namibia. We appreciate the excellent work of the technical support staff in Berlin, Durham, Hamburg, Heidelberg, Palaiseau, Paris, Saclay, and in Namibia in the construction and operation of the equipment. The author thanks the organizers for their kind invitation to this inspiring workshop.

References

Acciari, V. A., et al. 2009, Sci., 325, 444
Acciari, V. A., et al. 2008, ApJ, 679, 1427
Acero, F., et al. 2009, Sci., 326, 1080

Aharonian, F., et al. 2003, A&A, 403, L1
Aharonian, F., et al. 2009a, A&A, 502, 749
Aharonian, F., et al. 2009b, ApJ, 696, L150
Aharonian, F., et al. 2009c, ApJ, 695, L40
Aharonian, F., et al. 2005a, A&A, 430, 865
Aharonian, F., , et al. 2007a, ApJ, 664, L71
Aharonian, F., et al. 2006a, A&A, 457, 899
Aharonian, F., et al. 2006b, A&A, 455, 461
Aharonian, F., et al. 2006c, Nature, 440, 1018
Aharonian, F., , et al. 2005b, A&A, 442, 895
Aharonian, F., , et al. 2007b, A&A, 470, 475
Aharonian, F., et al. 2006d, Sci., 314, 1424
Aharonian, F. A. 2000, New Astronomy, 5, 377
Aharonian, F. A., et al. 2002, A&A, 393, 89
Albert, J., et al. 2008, ApJ, 674, 1037
Aleksić, J., et al. 2011a, A&A, 530, A4+
Aleksić, J., et al. 2011b, ApJ, 730, L8+
Blandford, R. D. & Znajek, R. L. 1977, MNRAS, 179, 433
Chadwick, P. M., et al. 1999, ApJ, 513, 161
Cooke, B. A., Lawrence, A., & Perola, G. C. 1978, MNRAS, 182, 661
Costamante, L., et al. 2001, å, 371, 512
Degrange, B., Superina, G., Giebels, B., & Volpe, F. 2008, in Blazar Variability across the Electromagnetic Spectrum
Forman, W., et al. 1978, ApJSupplement, 38, 357
Fortin, P. et al. 2011, to appear in PoS(Texas 2011), Heidelberg, Germany
Giebels, B., Aharonian, F., & Sol, H. 2010, ArXiv e-prints
Giebels, B. & Degrange, B. 2009, A&A, 503, 797
Griffiths, R. E., Briel, U., Chaisson, L., & Tapia, S. 1979, ApJ, 234, 810
Harris, R., et al. 2009, New Journal of Physics, 11, 123022
HESS Collaboration, Abramowski, A., , et al. 2010, A&A, 516, A56+
Krawczynski, H., et al. 2001, ApJ, 559, 187
Mannheim, K. 1993, A&A, 269, 67
Mücke, A. & Protheroe, R. J. 2001, Astroparticle Physics, 15, 121
Pohl, M. & Schlickeiser, R. 2000, A&A, 354, 395
Primack, J., Bullock, J., Summerville, R., & MacMinn, D. 1999, Astroparticle Physics, 11, 93
Punch, M., et al. 1992, Nature, 358, 477
Raue, M. 2011, to appear in Beamed and Unbeamed Gamma-rays from Galaxies, Muoino, Finnland
Rees, M. J. 1984, ARA&A, 22, 471
Rieger, F. 2011, in Multifrequency Behaviour of High Energy Cosmic Sources, F. Giovannelli & L. Sabau-Graziati (eds.), Mem. SAIt. Vol. 83 n. 1 (in press).
Schwartz, D., et al. 1989, "in Lecture Notes in Physics, edited by L. Maraschi, Maccacaro, T. and Ulrich, H. (Springer Berlin), Vol. 334, p. 211"
Schwartz, D. A., et al. 1979, ApJ, 229, L53
Sikora, M. & Madejski, G. 2001, AIP CONF.PROC., 558, 275
Stecker, F. W., de Jager, O. C., & Salamon, M. H. 1992, ApJ, 390, L49
Tluczykont, M., et al. 2010, A&A, 524, A48+
Urry, C. M. & Padovani, P. 1995, PASP, 107, 803